

Article

# Intraoral Temperature Triggered Shape-Memory Effect and Sealing Capability of A Transpolyisoprene-Based Polymer

Gakuji Tsukada <sup>1,\*</sup>, Ryuzo Kato <sup>2,†</sup>, Masayuki Tokuda <sup>1,†</sup> and Yoshihiro Nishitani <sup>1,†</sup>

Received: 20 September 2015 ; Accepted: 29 October 2015 ; Published: 9 November 2015

Academic Editor: Wei Min Huang

<sup>1</sup> Department of Restorative Dentistry and Endodontology, Kagoshima University Graduate School of Medical and Dental Sciences, 8-35-1 Sakuragaoka, Kagoshima 890-8544, Japan; mas-tok@dent.kagoshima-u.ac.jp (M.T.); nishi@dent.kagoshima-u.ac.jp (Y.N.)

<sup>2</sup> Department of Information Science and Biomedical Engineering, Graduate School of Science and Engineering, Kagoshima University, 1-21-40, Korimoto, Kagoshima 890-0065, Japan; ryu@ibe.kagoshima-u.ac.jp

\* Correspondence: tsukada@dent.kagoshima-u.ac.jp; Tel./Fax: +81-99-275-6192

† These authors contributed equally to this work.

**Abstract:** In dentistry, pure gutta-percha (*trans*-1,4-polyisoprene (TPI)) is widely used as a main component of root canal filling materials. TPI has an interesting shape memory formed through cross-linking, and this characteristic is expected to be very effective for development of novel dental treatments; in particular, modification of the shape recovery temperature to the intraoral temperature (37 °C) will enhance the applicability of the shape-memory effect of TPI in root canal filling. In this study, trial test specimens consisting of varying proportions of TPI, *cis*-polyisoprene, zinc oxide, stearic acid, sulfur and dicumyl peroxide were prepared and the temperature dependence of their shape recovery, recovery stress and relaxation modulus were measured. Additionally, their sealing abilities were tested using glass tubing and a bovine incisor. As the ratio of cross-linking agent in the specimens increased, a decrease in recovery temperature and an increase in recovery stress and recovery speed were observed. In addition, the test specimen containing the highest concentration of cross-linking agent showed superior sealing ability under a thermal stimulus of 37 °C in both sealing ability tests.

**Keywords:** shape-memory polymer; gutta-percha; *trans*-1,4-polyisoprene; root canal filling material; thermal property; crystallinity; sealing ability; *cis*-polyisoprene

## 1. Introduction

In dentistry, gutta-percha is one of the most popular materials for obturating the root canal space. This root canal filling treatment is one of the most important procedures in endodontic treatment, because microleakage of the root canal resulting from an inadequate seal can permit the passage of bacteria, fluids, and chemical substances [1,2]. Lateral condensation and the warmed gutta-percha technique are the main root canal filling methods performed clinically using gutta-percha [3–5]. The lateral condensation technique, which fills the root canal space using one master gutta-percha point and a number of accessory gutta-percha points with side-to-side filling using a dental spreader, has been widely used clinically for many years. The size of the master point is usually identical to that of the K-file used for final enlargement of the root canal, and the apical seat is then prepared slightly above the apical foramen to prevent extrusion of the master point from the apical foramen. Resistance (tug-back) upon withdrawing the master point inserted up to the apical seat is

used to confirm whether the tip of the master point is suitable for the shape of the enlarged root canal. Additionally, this technique is always used in combination with a root canal sealer. The advantage of the technique is easy control of the filling operation, and hence the method is still widely taught in dental schools [6]. However, it is difficult to fit the master points to the irregular shape of the root canal using only tug-back resistance, and poor sealing has been reported [7]. The warmed gutta-percha technique, in which the thermoplasticity of the material is used to obturate the root canal space, has been developed to overcome the disadvantages of the lateral condensation technique [8,9]. Since the proposal of vertical condensation of warmed gutta-percha [10], injectable thermoplasticized gutta-percha has been introduced [11] and a variety of techniques using warmed gutta-percha have been developed. Several studies have compared the sealing ability of the warmed gutta-percha and lateral condensation techniques [4,12,13]. However, it has been found that warmed gutta-percha techniques are not necessarily superior to the lateral condensation procedure [14,15], and the use of root canal sealer is frequently required in warmed gutta-percha methods [16,17]. In addition, problems such as shrinkage during setting [18–20] and overextension of the gutta-percha and the root canal sealer from the apical foramen [21,22] have been reported. As a consequence, warmed gutta-percha techniques have not yet replaced the lateral condensation method.

Gutta-percha is a composite material [23–25], and pure gutta-percha (*trans*-1,4-polyisoprene (TPI)) has been used as the main component of dental gutta-percha for a number of years because of its very low toxicity [26,27] and ease of handling [6]. TPI is incorporated into gutta-percha in a non-cross-linked state. TPI is a crystalline polymer [28–32] that is easily cross-linked using sulfur or peroxide, with mechanical properties dependent on its crystallinity [20,23]. These properties lead to TPI demonstrating interesting shape-memory properties [31–37], and this shape-memory polymer has been commercialized under the product name SMP-2 (Kuraray Corporation, Kashima, Japan).

In our previous study [32], we confirmed the shape-memory capacity of SMP-2, and this function was expected to be effective for close filling of the root canal. However, the shape recovery temperature of SMP-2 is somewhat (about 10–15 °C) higher than the intraoral temperature (37 °C) [32] and application of SMP-2 as a root canal filling material has been found to be difficult. Adjustment of the shape recovery temperature to the intraoral temperature (37 °C) would greatly improve the operability of SMP-2 as a root canal filling material. Hence, confirmation of the possibility of adjustment of the shape recovery temperature to 37 °C for various TPI composites, and examination of the sealing ability using the shape-memory effect of TPI-based polymers is necessary.

The purpose of this study was to prepare trial samples consisting of a TPI-based shape-memory polymer and examine methods for adjusting the thermal properties of this polymer to identify a formulation that yielded shape recovery at 37 °C. The sealing ability of the shape-memory polymers was also measured using two methods: glass tubing and a bovine incisor. The bovine incisor was used to test both the lateral condensation method and the warmed gutta-percha for a comparison of sealing ability.

## 2. Experimental Section

### 2.1. Shape-Memory Polymer Preparation

Trial materials for the study were prepared, and the component ratios of the ingredients are shown in Table 1. TPI (TP-301, Kuraray Corporation, Kyoto, Japan) was used as the main base polymer, and *cis*-1,4-polyisoprene (Sigma-Aldrich Corporation, St. Louis, MO, USA [CPI]) was used as the co-cross-linking polymer. Zinc oxide and stearic acid (both from Wako Pure Chemical Industry, Ltd., Osaka, Japan) were used as accelerator activators, and sulfur and dicumyl peroxide (both from Nacalai Tesque Inc., Kyoto, Japan) were used as cross-linking agents. TPI, zinc oxide, stearic acid is used as a component of gutta-percha. The amounts of zinc oxide and stearic acid were identical for all specimens (Table 1), whereas the amounts of TPI, CPI, sulfur and dicumyl peroxide were changed for each specimen. Specimen TPI:100-S:0.5 material was prepared as a standard material,

and test specimens were prepared by stepwise variation of the proportions of TPI and CPI to yield specimens TPI:85-S:0.5, TPI:70-S:0.5 and TPI:50-S:0.5. A further set of specimens was prepared by stepwise variation of the quantity of cross-linking agents added (sulfur and dicumyl peroxide) to yield specimens TPI:100-S:0.75, TPI:100-S:1.0 and TPI:100-S:1.25. Specimen compositions are shown in Table 1.

**Table 1.** Test materials and component ratios of their ingredients. The compound ingredients are given as parts per hundred by weight of the rubber polymer.

Code	TPI:100-S:0.5	TPI:85-S:0.5	TPI:70-S:0.5	TPI:50-S:0.5	TPI:100-S:0.75	TPI:100-S:1.0	TPI:100-S:1.25
<i>Trans</i> -1,4-polyisoprene	100	85	70	50	100	100	100
<i>Cis</i> -1,4-polyisoprene	0	15	30	50	0	0	0
Zinc oxide	30	30	30	30	30	30	30
Stearic acid	1	1	1	1	1	1	1
Sulfur	0.5	0.5	0.5	0.5	0.75	1.0	1.25
Dicumyl peroxide	3	3	3	3	4.5	6.0	7.5

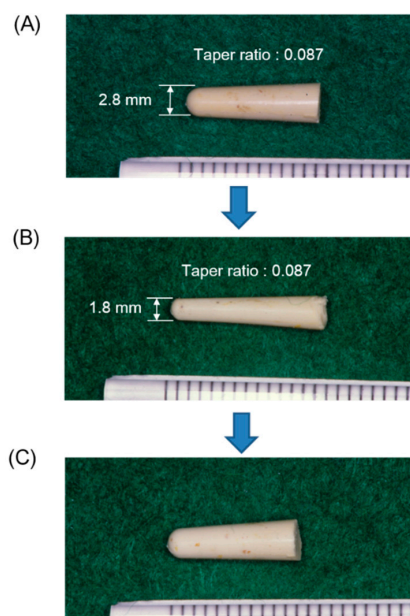


**Figure 1.** Photograph of the trial point: (A) original shape; (B) deformed shape; and (C) recovery shape.

Test specimens were prepared in almost accordance with a previously reported method [32]. First, non-cross-linked compounds were prepared by kneading the raw ingredients using a rubber roller at  $75 \pm 5$  °C for 11 min. Split metal molds were prepared to form cylindrical test specimens and trial points (Figure S1A,B in Supplementary Materials). The non-cross-linked compound was heated at 90 °C for 10 min to soften the material, placed in the metal mold, and pressed at 196 N. The mold containing the non-cross-linked compound was heated from 24 to 150 °C for 15 min in an oven and then held at 150 °C for 30 min under a nitrogen gas atmosphere to cross-link the TPI and CPI. The mold was then cooled to room temperature and the sample was removed from the mold. Hence, cylindrical test specimens (6.0 mm diameter, 9.5 mm length) (Figure S2A, Supplementary Materials) and trial points having a 0.087 taper ratio (Figure 1A) were prepared. The tip of the trial point was spherically formed and its diameter was 2.8 mm. Thermal property measurements and a sealing ability test using glass tubing were performed on each cross-linked cylindrical test specimen, and a sealing ability test using a bovine incisor was performed on the trial point. For measurement of the thermal properties, the original shape (Figure S2A, Supplementary Materials) was compressed to be deformed as shown in Figure S2B, Supplementary Materials and subsequently allowed to

recover, as shown in Figure S2D, Supplementary Materials. In contrast, for the sealing ability test, the deformed shape fixation and shape recovery patterns shown in Figure S2A,C,D (Supplementary Materials) were used. Similar results were obtained from five replicate determinations and median values are reported.

### 2.2. Measurement of Shape Recovery Ratio at a Fixed Constant Temperature for the Standard Material

The shape recovery of the TPI:100-S:0.5 material prepared as the standard was investigated under a range of temperature conditions. Shape recovery ratios were measured from 37–55 °C and the test procedure was as follows: the axial length of the test specimen was measured at 24 °C (original length, Figure S2A, Supplementary Materials). The specimen was then softened by heating in a water bath at 90 °C for 3 min, then axially compressed by 30%. Cooling the specimen in a water bath at 0 °C fixed the compressed dimensions. The specimen was then taken out of the water and allowed to equilibrate to 24 °C to stabilize the dimensions. The length of the deformed specimen was then measured (deformed length, Figure S2B, Supplementary Materials). The specimen was heated in a thermostat-controlled box maintained at a constant temperature. After heating for 10 min at each temperature, the test specimen was removed from the box and immediately immersed in a water bath at 0 °C for 10 min. The specimen was then placed at room temperature at 24 °C to equilibrate. The length of the test specimen was remeasured (recovery length, Figure S2D, Supplementary Materials) and the shape recovery ratio (SRR) was calculated as follows:

$$SRR (\%) = \frac{L_r - L_d}{L_0 - L_d} \times 100 \quad (1)$$

where  $L_r$  = recovery length,  $L_d$  = deformation length and  $L_0$  = original length.

### 2.3. Measurement of Shape Recovery under A Constant Rate Rising Temperature

All cylindrical test specimens were softened by heating in a water bath at 90 °C for 3 min and then axially compressed by 30% in length. Following this compressive deformation, the dimensions were fixed by cooling in a water bath at 0 °C. The test specimen was removed from the water bath and allowed to warm to 10 °C (Figure S2B, Supplementary Materials), then heated from 10–80 °C at 1.0 °C/min. Changes in length were measured using a laser displacement meter (LC-2100; Keyence Corporation, Osaka, Japan) across a range of temperatures to investigate the shape recovery from the deformed shape.

### 2.4. Measurement of Recovery Stress under a Constant Rate Rising Temperature

The stress generated by shape recovery from the deformed shape was measured using a compression testing machine (AG-100; Shimadzu Corporation, Kyoto, Japan). The test specimens were softened by heating in a water bath at 90 °C for 3 min, then axially compressed by 30% in length. The compressive deformation was fixed by cooling in a water bath at 0 °C for 10 min and the test specimen was removed from the water bath (Figure S2B, Supplementary Materials). The test specimen was then placed on a table installed in the testing machine, surrounded by a temperature-controlled box, and allowed to warm to 10 °C. An indenter, which was connected to the load cell, was placed in contact with the top of the deformed test specimen. The position of the indenter was fixed while the test specimen was heated at a rate of 1.0 °C/min from 10–80 °C. The stresses generated by heating were measured.

### 2.5. Measurement of Relaxation Modulus at a Fixed Constant Temperature

The relaxation modulus was measured using a compression testing machine (TG-50KN; Minebea Corporation Ltd., Nagano, Japan). All specimens were placed on a platen enclosed in a thermostat-controlled box; the temperature of the specimen was changed by changing the

temperature of the box. Measurements were made at constant temperatures in the range 4–80 °C. The compressive strain ( $\gamma$ ) was 0.05, the measurement time was 10 s, and the relaxation modulus ( $E_r(t)$ ) was calculated as follows:

$$E_r(t) = \frac{f(t)}{\gamma} \quad (2)$$

where  $f(t)$  is the compressive stress after  $t$  seconds from the start of the measurement. In this study,  $f(5)$  was used.

#### 2.6. Measurement of the Shape Recovery Ratio at a Fixed Constant Temperature of 37 °C

To examine the degree of shape recovery from the deformed shape at the intraoral temperature (37 °C), the shape recovery ratio of all specimens was measured at a constant temperature of 37 °C. The test procedure was as follows: the axial length of the specimen was deformed by 30% and fixed in the same way as described in Section 2.2. The axial length of the specimen was measured at 24 °C (original length and deformed length, Figure S1A,B, Supplementary Materials), and no dimension changes were recorded. The specimen was heated in a thermostat-controlled box at 37 °C. After heating for each time period (1–10 min), the specimen was removed from the box and immediately immersed in a water bath at 0 °C for 10 min. The specimen was then removed from the water bath and again placed at 24 °C to equilibrate. The length of the test specimen was remeasured (recovery length), and the shape recovery rate (SRR) at each time was calculated as given by Equation (1).

#### 2.7. Sealing Ability Test Using Glass Tubing

Cross-linked cylindrical specimens (Figure S2A, Supplementary Materials) were softened by heating in a water bath at 90 °C for 3 min, then inserted into a glass tube (inner diameter 4.6 mm) and cooled in a water bath at 0 °C for 10 min to fix the deformation. The specimen in the glass tube was removed from the water bath, and the deformed test specimen was removed from the glass tube. The deformed specimen was then exposed at room temperature (24 °C) and allowed to equilibrate to stabilize the dimensions, and the fixation of the deformed shape was confirmed (Figure S2C, Supplementary Materials).

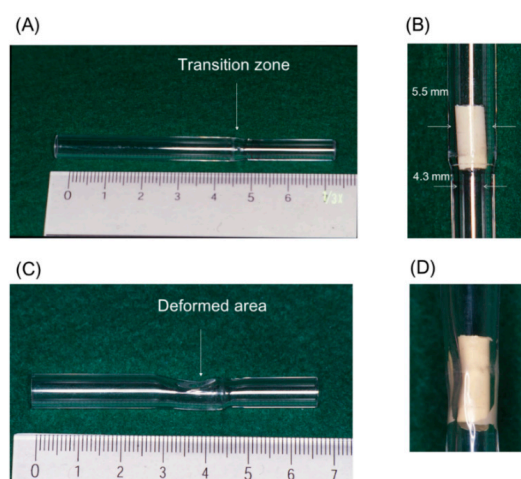


**Figure 2.** Photograph of the glass tube for the sealing test: (A) glass tube; (B) glass tube with deformed test specimen inserted; (C) flattened deformed glass tube; and (D) flattened deformed glass tube with deformed test specimen inserted.

Another glass tube (inner diameter 5.5 mm in the upper section and 4.3 mm in the lower) was prepared for this test (Figure 2A) and stored in an incubator at 37 °C. A test specimen (diameter 4.6 mm) was inserted into the larger section of the tube and pushed up to the transition zone to the

smaller inner diameter. This transition zone was intended to model the apical seat and insertion of the deformed test specimen was stopped at this point (Figure 2B). The specimen in the glass tube was then compressed axially at 0.981 N for 5 min using an indenter, in an incubator at 37 °C (Figure 3A,B). If the shape of the test specimen was recovered by the thermal stimulus at 37 °C, the test specimen thus sealed the glass tube (Figure 3C,D). In addition, the sealing ability test was performed using a deformed flattened glass tube (Figure 2C). This glass tube was prepared by pressing the original glass tube (Figure 2A) under heat until just before the deformed specimen could no longer be inserted up to the transition zone (Figure 2D).

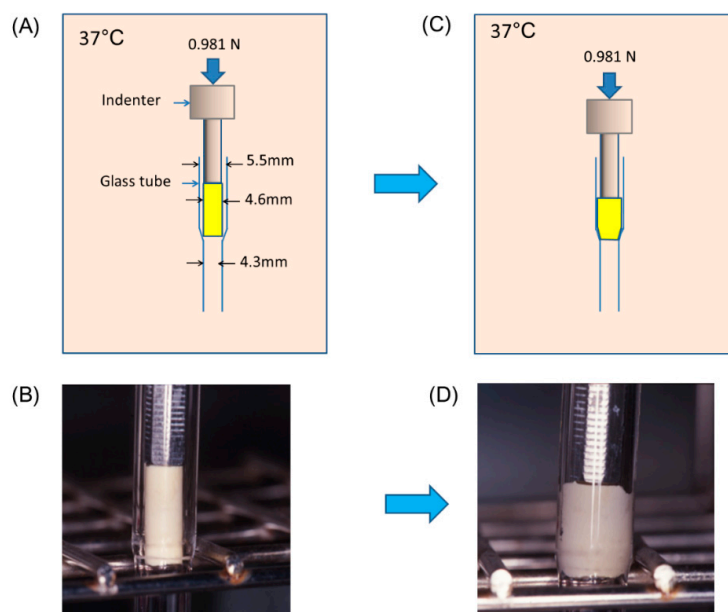


**Figure 3.** (A) Schematic representation of the filling method for the glass tube; (B) photograph of the filling method for the glass tube; (C) schematic representation after filling the glass tube with the test specimen; and (D) photograph after filling the glass tube with the test specimen.

As shown in Figure 4A,B, the sealing ability of the specimen was tested by immersion of the lower, wider end of the tube containing the specimen in water at 37 °C, while the upper end was filled with 1% fuchsin basic solution (Nacalai Tesque Inc., Kyoto, Japan). Electrical resistance was measured using a digital multimeter to evaluate water leakage.

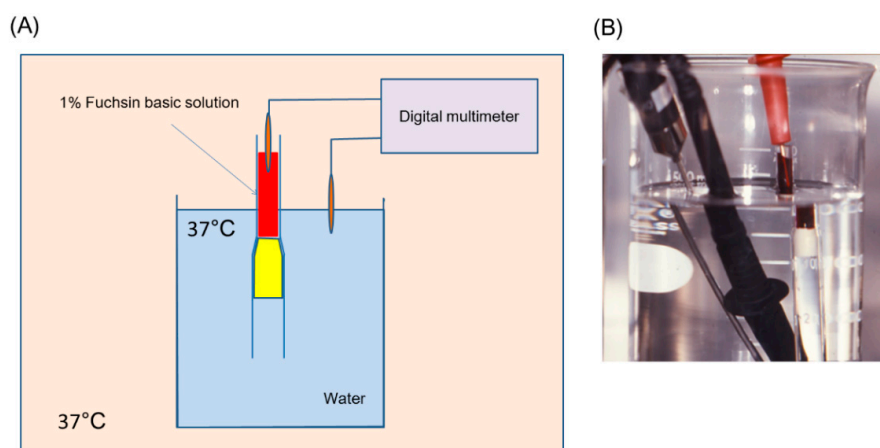


**Figure 4.** Sealing ability test: (A) schematic representation and (B) photograph.

### 2.8. Sealing Ability Test Using Bovine Incisor

To examine the sealing ability in an environment similar to the human root canal, the sealing ability test was performed using the root canal of a bovine incisor, which has a shape and properties resembling that of the root canal of the human tooth. The size of the trial point was referenced to that of the root canal of the bovine incisor, and only the TPI:100-S:1.25 material sample was prepared for this experiment. The trial point (Figure 1A) was softened by heating in a water bath at 90 °C for 3 min, and then inserted into the metal mold (Figure S1C, Supplementary Materials) and compressed using an indenter for deformation. Following deformation, the dimensions were fixed by cooling in a water bath at 0 °C for 3 min. The mold was removed from the water bath and the trial point was removed from the mold and placed at room temperature at 24 °C. No change in dimensions was recorded (Figure 1B). The deformed points had a 0.087 taper ratio and its tip was formed spherical (1.8 mm diameter). Fresh bovine incisors were obtained. The crowns, pulp and periodontal membrane were removed and the root canals enlarged using a steel dental bur until the deformed point (Figure 1B) could be inserted without resistance into the root canal and stopped at the apical seat. Nail varnish was then applied to the entire root surface excluding the apical foramen (Figure 5).

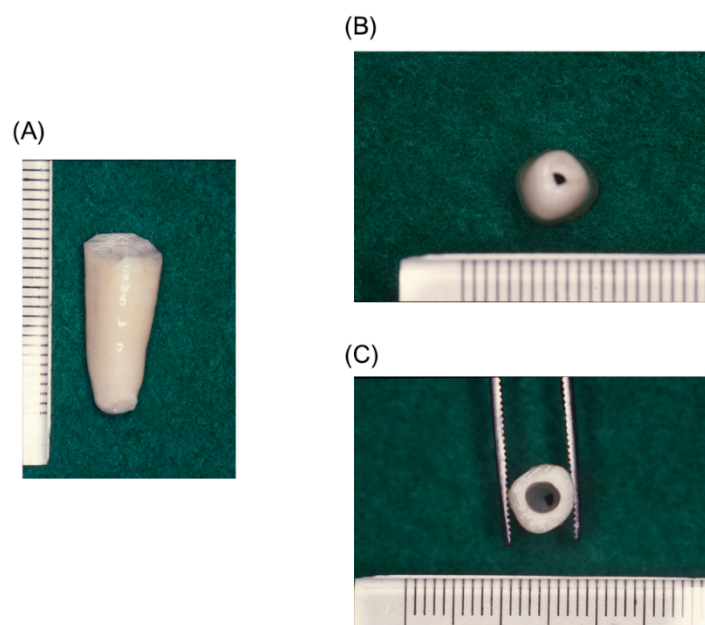


**Figure 5.** Photograph of the root of the bovine incisor prepared for the sealing-ability test with the trial point: (A) lateral side; (B) apical side; and (C) cervical side.

The deformed trial point (Figure 1B) was inserted into the root canal (Figure 6A), which was stored in an incubator at 37 °C, and compression was maintained using an indenter for 5 min at 0.981 N. The root canal space was filled after recovery of the trial point (Figure 6B), and root canal sealer was not used together. For comparison with the current preferred root canal filling method performed clinically, the sealing ability test was also performed on bovine root canals filled using the lateral condensation technique and the warmed gutta-percha technique. To compare the sealing ability of the gutta-percha, root canal sealer was not used. For the lateral condensation technique, the root canal of the bovine incisor was enlarged to the size of the #140 K-file and the apical seat added, then the root canal was irrigated with 3%EDTA solution and 3% sodium hypochlorite solution. A #140 master point (GC Corporation, Tokyo, Japan) was then inserted into the root canal and tug-back confirmed (Figure 6C). In this study, the sealing ability to the apical foramen by the master point only, confirmed by tug-back, was examined. For the warmed gutta-percha technique, the root canal was enlarged and irrigated in a similar manner, and the root canal of a bovine

incisor was filled with three kinds of gutta-percha: Obtura II (Obtura Corporation, Fenton, MO, USA), Obturation Gutta Hard (Toyo Chemical Corporation, Tokyo, Japan) and Ultrafil Regular Set (Hygenic Corporation, Akron, OH, USA). The root canal of the bovine incisor was filled with these gutta-perchas using the respective dedicated devices in accordance with the manufacturers' instructions. The filled root was immersed in a 1% fuchsin solution without soaking the cut surface (Figure 7). The immersed root was taken out (Figure 7B) after 24 h for the lateral condensation method, at 4 days for the warmed gutta-percha method, and at 10 days for the trial point. After that, the root was cut longitudinally using a low-speed diamond saw (Isomet, Buehler Co., Lake Bluff, IL, USA) and the sealing ability was confirmed using a dye penetration.

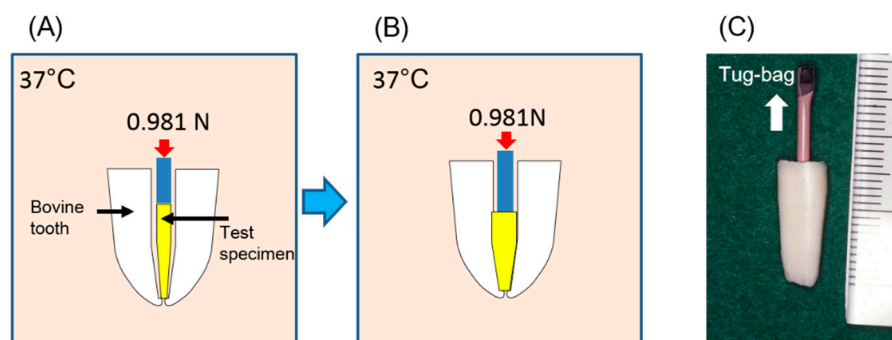


**Figure 6.** (A) Schematic representation of the filling method for the root canal of the bovine incisor; (B) schematic representation after filling the root canal of the bovine incisor; and (C) confirmation of tug-back.

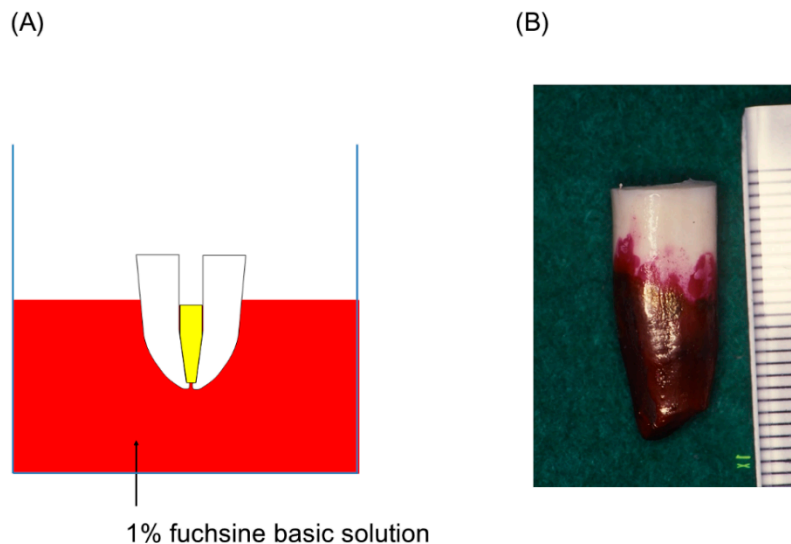


**Figure 7.** (A) Schematic representation of filled root of bovine incisor immersed in 1% fuchsin basic staining solution; and (B) photograph of the root of bovine incisor after removal from 1% fuchsin basic staining solution.

### 3. Results

#### 3.1. Shape Recovery Ratio under A Fixed Constant Temperature for the Standard Material

The shape recovery ratio of the TPI:100-S:0.5 standard material at each fixed constant temperature is shown in Figure 8. Shape recovery was not observed between 37 and 43 °C.

From 44 °C, the shape recovery ratio increased with temperature and reached almost 100% at over 53 °C (Figure 8).

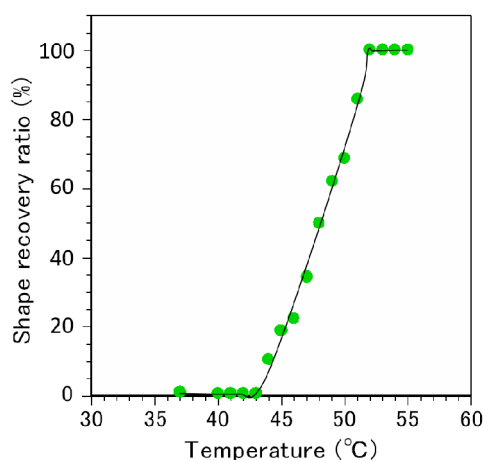


Figure 8. Shape recovery ratio under a fixed constant temperature for the standard material.

### 3.2. Shape Recovery under a Constant Rate Rising Temperature

The changes in shape recovery for the different proportions of TPI to CPI are shown in Figure 9A and for different proportions of cross-linking agent in Figure 9B. In all specimens, the length of each specimen increased slightly at lower temperatures (Figure 9A,B). In Figure 9A, marked increases in length are observed from 24 to 34 °C for TPI:50-S:0.5, 30 to 38 °C for TPI:70-S:0.5, 32 to 40 °C for TPI:85-S:0.5 and 33 to 42 °C for TPI:100-S:0.5. As the proportion of CPI increased, the shape recovery temperature at which a marked increase in length was observed decreased. In Figure 9B, marked increases in length were observed at 22 to 29 °C for TPI:100-S:1.25, 24 to 31 °C for TPI:100-S:1.0 and 27 to 34 °C for TPI:100-S:0.75. As the proportion of cross-linking agent increased, the shape recovery temperature at which a marked increase in length was observed decreased. At higher temperatures, each specimen behaved similarly. Because a significant changes were not observed in the measured values above 60 °C, they were not shown in Figure 9.

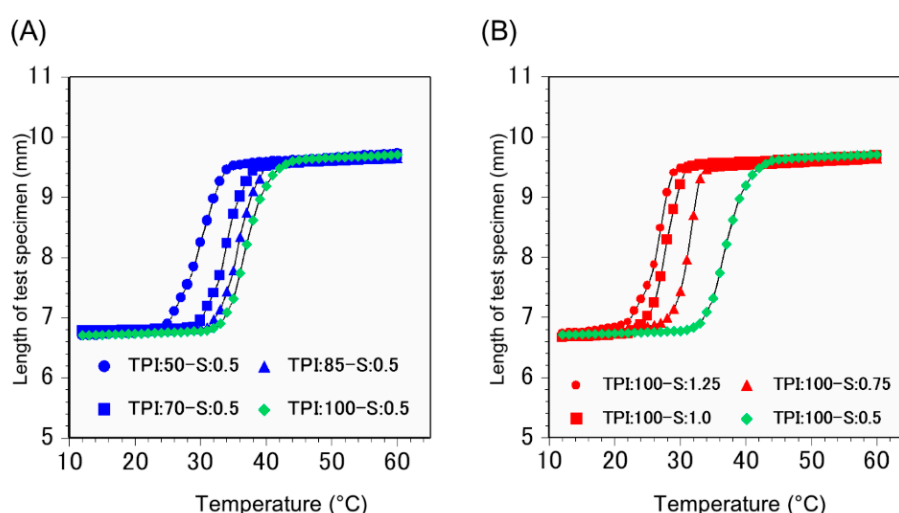
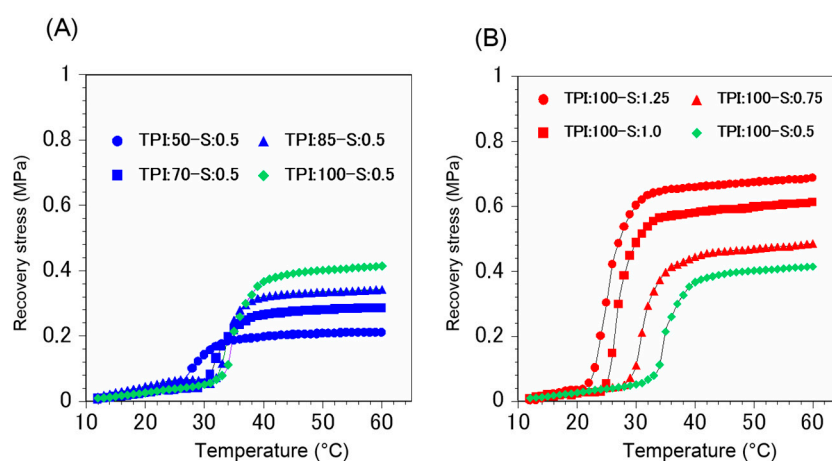


Figure 9. Changes in shape recovery from deformation as a function of temperature for (A) TPI:50-S:0.5, TPI:70-S:0.5, TPI:85-S:0.5 and TPI:100-S:0.5 (various proportions of TPI to CPI); and (B) TPI:100-S:1.25, TPI:100-S:1.0, TPI:100-S:0.75 and TPI:100-S:0.5 (various amounts of cross-linking agents).

### 3.3. Recovery Stress under a Constant Rate Rising Temperature

Changes in recovery stress generated through recovery from the deformed shape are shown in Figure 10A,B. Figure 10A shows the effect of changing the proportion of TPI to CPI, and Figure 10B shows the effect of changing the amount of cross-linking agent. In all specimens, recovery stress increased slightly at lower temperatures. In specimens of varying polymer composition, marked increases in recovery stress were observed in the following temperature ranges: 26 to 33 °C for TPI:50-S:0.5, 30 to 37 °C for TPI:70-S:0.5, 32 to 38 °C for TPI:85-S:0.5 and 33 to 40 °C for TPI:100-S:0.5 (Figure 10A). At higher temperatures, the highest recovery stress value was seen in test material TPI:100-S:0.5, followed by TPI:85-S:0.5, TPI:70-S:0.5, and TPI:50-S:0.5 (Figure 10A). In specimens with varying amounts of cross-linking agent, marked increases in recovery stress were observed in the following temperature ranges: 22 to 30 °C for TPI:100-S:1.25, 25 to 33 °C for TPI:100-S:1.0, and 29 to 36 °C for TPI:100-S:0.75 (Figure 10B). At higher temperatures, the highest recovery stress value was seen in test material TPI:100-S:1.25, followed by TPI:100-S:1.0, TPI:100-S:0.75, and TPI:100-S:0.5. As the proportion of CPI increased, recovery stress decreased at high temperatures (Figure 10A). In contrast, as the proportion of cross-linking agent increased, recovery stress increased at high temperatures (Figure 10B). Because a significant changes were not observed in the measured values above 60 °C, they were not shown in Figure 10.



**Figure 10.** Changes in shape recovery stress as a function of temperature for (A) TPI:50-S:0.5, TPI:70-S:0.5, TPI:85-S:0.5 and TPI:100-S:0.5 (varying proportion of TPI to CPI); and (B) TPI:100-S:1.25, TPI:100-S:1.0, TPI:100-S:0.75 and TPI:100-S:0.5 (various amounts of cross-linking agents).

### 3.4. Relaxation Modulus under a Fixed Constant Temperature

Changes in the relaxation modulus after 5 s ( $E_r(5)$ ) are shown in Figure 11A,B. Figure 11A shows the effect of changing the proportion of TPI to CPI, and Figure 11B shows the effect of changing the amount of cross-linking agent. In all specimens, a higher  $E_r(5)$  value was observed at lower temperatures. In specimens of varying polymer composition, marked decreases in  $E_r(5)$  were observed in the following temperature ranges: 22 to 40 °C for TPI:50-S:0.5, 26 to 42 °C for TPI:70-S:0.5, 28 to 42 °C for TPI:85-S:0.5 and 32 to 44 °C for TPI:100-S:0.5 (Figure 11A). At higher temperatures, the highest  $E_r(5)$  value was seen in test material TPI:100-S:0.5, followed by TPI:85-S:0.5, TPI:70-S:0.5, and TPI:50-S:0.5 (Figure 11A). In specimens with varying proportions of cross-linking agent, marked decreases in  $E_r(5)$  were observed in the following temperature ranges: 22 to 30 °C for TPI:100-S:1.25, 22 to 32 °C for TPI:100-S:1.0, and 24 to 44 °C for TPI:100-S:0.75 (Figure 11B). At higher temperatures, the highest  $E_r(5)$  value was seen in test material TPI:100-S:1.25, followed by TPI:100-S:1.0, TPI:100-S:0.75, and TPI:100-S:0.5. As the proportion of CPI increased,  $E_r(5)$  decreased at high temperatures (Figure 11A). In contrast, as the proportion of cross-linking agent increased,

$E_r(5)$  increased at high temperatures (Figure 11B). Because a significant changes were not observed in the measured values above 60 °C, they were not shown in Figure 11.

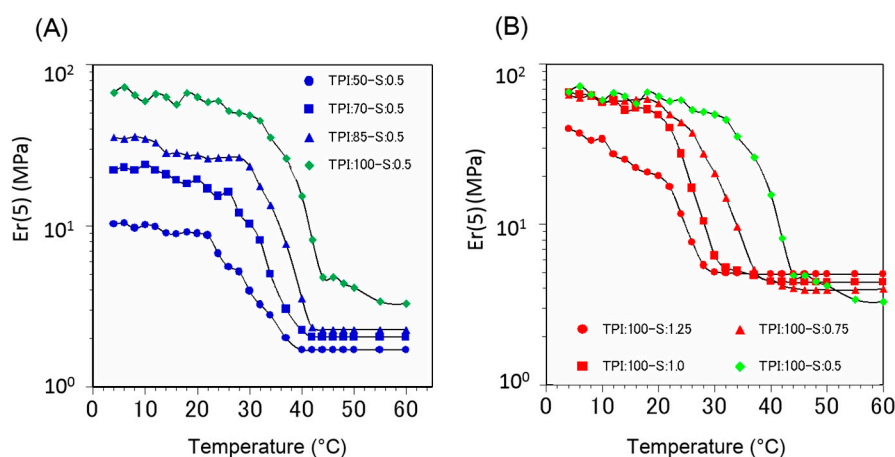


**Figure 11.** Changes in  $E_r(5)$  as a function of temperature for (A) TPI:50-S:0.5, TPI:70-S:0.5, TPI:85-S:0.5 and TPI:100-S:0.5 (varying proportion of TPI to CPI); and (B) TPI:100-S:1.25, TPI:100-S:1.0, TPI:100-S:0.75 and TPI:100-S:0.5 (various amounts of cross-linking agents).

### 3.5. Measurement of the Shape Recovery Ratio at 37 °C

The shape recovery ratio of all specimens at 37 °C is shown in Figure 12. The shape recovery ratio of specimen TPI:100-S:1.25 was highest and reached almost 100% after 4 min. The shape recovery ratio of TPI:100-S:1.0 reached almost 100% after 7 min. In contrast, specimens TPI:50-S:0.5 and TPI:70-S:0.5 showed a slow shape recovery speed, and a 100% recovery ratio was not reached after 10 min. Ratios of 67.7% for TPI:50-S:0.5 and 60.0% for TPI:70-S:0.5 were reached after 10 min (Figure 12). TPI:85-S:0.5, TPI:100-S:0.75 and TPI:100-S:0.5 showed no recovery at 37 °C.

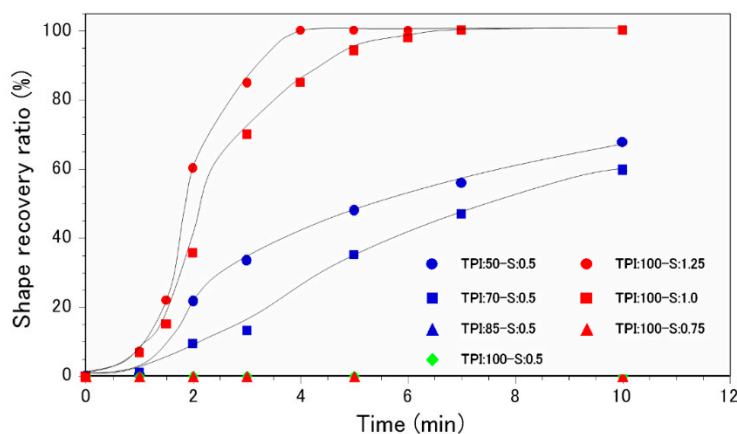


**Figure 12.** Shape recovery ratio of all materials under a fixed constant temperature of 37 °C.

### 3.6. Sealing Ability using Glass Tubing

A photograph of the sealing ability test using the glass tube without deformation is shown in Figure 13A. For test material TPI:100-S:1.25, no dye penetration was observed after three months and one year (Figure 13A,B). A photograph of the sealing ability test using the deformed glass tube is shown in Figure 13C. No dye penetration was observed after one month, indicating no water leakage. In addition, electrical insulation was confirmed after three months, indicating no water leakage.

For other test materials, dye penetration and water leakage were observed immediately after the start of the test.

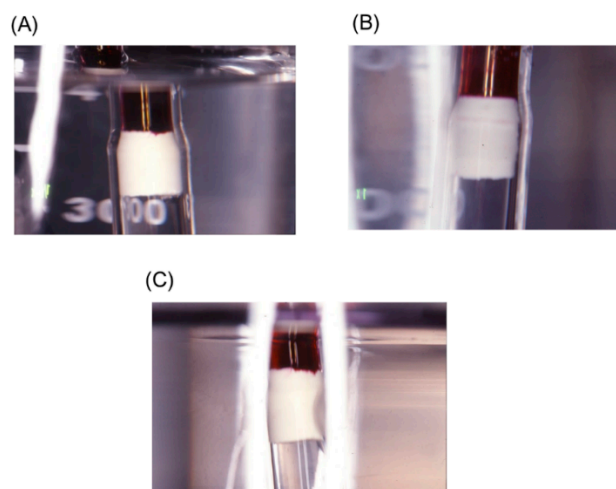


**Figure 13.** Photograph of glass tube sealed by polymer shape recovery: (A) after three months; and (B) after one year; (C) photograph of the flattened deformed glass tube sealed by polymer shape recovery after one month.

### 3.7. Sealing Ability using a Bovine Incisor

Photographs of the sealing ability test using a bovine incisor are shown in Figures 14 and 15. For the lateral condensation method, dye penetration was observed in the entire root canal after 24 h (Figure 14A). For the warmed gutta-percha method, dye penetration length from apical foramen of  $6.52 \pm 0.12$  h for Obtura II,  $2.41 \pm 0.66$  h for Obturation Gutta Hard and  $2.64 \pm 0.37$  h for Ultrafil Regular Set (Figure 14B–D) were observed after four days. In contrast, for the trial TPI:100-S:1.25 point, almost no dye penetration was observed after 10 days (Figure 15A–C). The trial point can adapt to a variety of root canal shapes such as a relatively regular tubular root canal (Figure 15A), a gradually tapered root canal (Figure 15B) and a steeply tapered root canal (Figure 15C). In addition, root fracture by recovery stress was not observed in any of the roots.

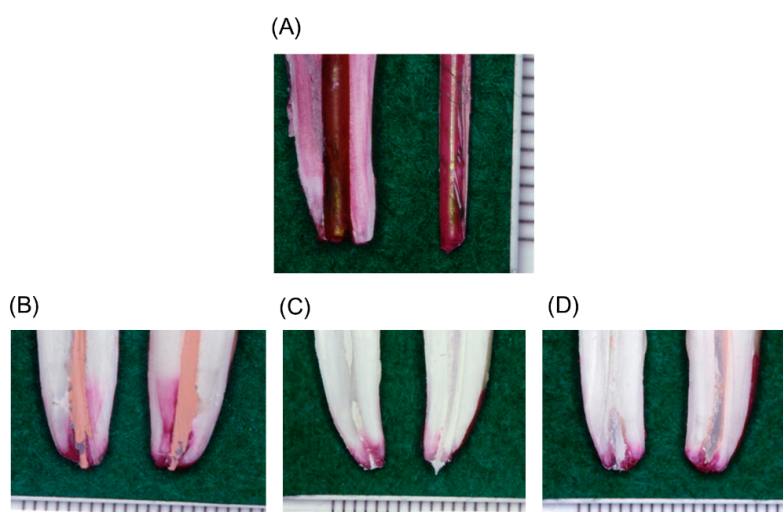


**Figure 14.** Photograph of the results of the dye penetration test after four days: (A) lateral condensation method, and warmed gutta-percha method (B) for Obtura II; (C) for Obturation Gutta Hard; and (D) for Ultrafil Regular Set.

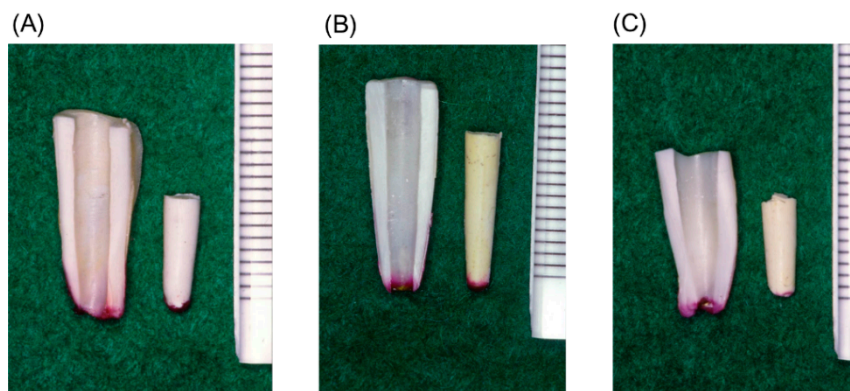


**Figure 15.** Photograph of the results of the dye-penetration test for the trial point at 10 days: (A) Relatively regular tubular root canal; (B) gradually tapered root canal; and (C) steeply tapered root canal.

#### 4. Discussion

Most endodontic failures can be attributed to poorly obturated root canals [38,39]. Therefore, an important property of a root canal filling material is the ability to seal the internal space of the root canal tightly over a long period. In addition, any filling material should have excellent operability. The internal shape of the root canal cannot be observed directly; thus the root canal filling procedure relies strongly on the intuition of the dentist. Therefore, the development of a new root canal filling method that does not depend on the dentist's technique is needed. Additionally, dentists desire a new, easy method that will reliably seal the root canal. As such, we have sought a new root canal filling technique using gutta-percha to replace existing methods using lateral condensation or warmed gutta-percha.

In our previous study, we confirmed the shape-memory capacity of SMP-2, a TPI-based polymer [32]. For ideal clinical application of shape-memory polymer as a root canal filling material, the shape deformation of the polymer should be fixed long-term at refrigeration temperature, the deformed shape should be maintained during dental treatment at room temperature, and recovery to the original memorized shape should occur upon exposure to the intraoral temperature (37 °C). Furthermore, shape recovery should be relatively rapid and the material should push against the root canal wall gently to seal it permanently without root fracture. Therefore, we sought to identify formulation parameters to alter the thermal properties of this polymer. In this study, TPI:100-S:0.5 was prepared as a standard material, with components and content ratios determined with reference to Ishii's report [31], to a study of SMP-2 [32] and to the components of commercial gutta-percha products for root canal filling material [23–25]. For TPI:100-S:0.5, the temperature at which the shape recovery ratio began to increase was 44 °C, and 100% shape recovery within 10 min was observed at over 52 °C (Figure 8). Based on these results, since it was not possible to induce shape recovery at the intraoral temperature using this composition, the composition was changed to attempt to decrease the shape recovery temperature.

A previous study showed that co-cross-linking with CPI decreases the shape recovery temperature of cross-linked TPI-based polymers [31]. TPI and CPI are *cis-trans* isomers of polyisoprene, which contains double bonds; the two polymers can therefore be co-cross-linked. Although the chemical formula of these polymers is identical, their properties are significantly different. The polymer form of TPI is relatively elongated, so polymer strands are close together and easily cohere to form crystalline structures [28–32]. This crystallization of TPI can resist forces that return the material to its original shape, memorized in the cross-linking reaction [31,32]. In contrast, CPI, or natural rubber, is extremely flexible at the double bond, making the polymer structure irregular (non-crystalline), with many gaps between polymer strands; intermolecular forces

within CPI are weak. Also, TPI has a high elasticity at 37 °C through crystallization, while CPI appears more syrup-like at this temperature. The decrease in shape recovery temperature with increasing proportions of CPI (Figure 9A) is likely due to the weakened crystallization of TPI when co-cross-linked with CPI. However, compounding with CPI likely decreases the recovery stress (Figure 10A). In addition, the shape recovery speed was slow (Figure 12). The sealing ability test using glass tubing showed a poor seal, likely caused by these thermal properties. Thus, co-cross-linking TPI with CPI does not appear to be suitable method for creating a root canal filling material.

The other approach to altering the shape recovery temperature of the cross-linked TPI-based polymers was to vary the cross-linking density of TPI. Shape recovery of TPI-based polymers occurs by melting of the crystalline region, which fixed the deformation [32]. In Figure 8, the shape recovery temperature of the standard specimen was lower than that of the transition temperature (melting point: 67 °C) of TPI [30]. Based on these results, increasing the degree of cross-linking of TPI was expected to be effective in decreasing the transition temperature. As shown in Figure 9B, as the proportion of cross-linking agent increased, the shape recovery temperature decreased, and the recovery stress increased (Figure 10B). An increase in cross-linking points and tightening of the mesh structure inhibits the movement of TPI polymer strands and decreases the molecules that contribute to crystallization. Moreover, the forces that act to recover the original shape memorized by cross-linking become stronger. In addition, recovery stress increases (Figure 10B) and the shape recovery speed increases (Figure 12). Based on these results, this modification seemed promising for application as a root canal filling material. The results shown in Figures 9 and 10 were measured under a rising temperature at a constant rate of 1 °C/min. For TPI:100-S:0.5, the temperature range of marked increases in length (33 to 42 °C) and in recovery stress (33 to 40 °C) was lower than the constant temperature used for measurement of the shape recovery ratio (Figure 8). Under a rising temperature conditions (1 °C/min), it was presumed that the transition temperature was shifted to the low temperature side, because recrystallization of the specimen after the melting of the crystalline region was suppressed by more heat was supplied in order to raise the specimen temperature constantly (1 °C/min) against the supercooling phenomenon by the endothermic reaction with crystalline melting.

The results shown in Figures 8, 11 and 12 were measured under fixed temperature conditions. Specimen TPI:100-S:0.5 showed an increased shape recovery ratio at 44 °C (Figure 8), this temperature (44 °C) is the point at which the elastic modulus changed from a marked decrease to a slight decrease (Figure 11A,B). The crystallinity of TPI was considered to be almost melted at 44 °C, the TPI:100-S:0.5 material was presumed to exhibit rubber elasticity, shape recovery was spontaneously induced, and its recovery ratio increased with increasing temperature and rubber elasticity (Figure 8). One of the most important themes of this study was to identify a formulation of TPI polymer that yields shape recovery at 37 °C; the results shown in Figure 12 suggest these characteristics for test specimens TPI:50-S:0.5, TPI:70-S:0.5, TPI:100-S:1.25 and TPI:100-S:1.0. For TPI:100-S:1.25 and TPI:100-S:1.0, the elastic modulus at 37 °C had stabilized and the specimens had transformed into a rubber state (Figure 11B) and were presumed to be able to recover their shape spontaneously. In contrast, specimens TPI:50-S:0.5 and TPI:70-S:0.5 had an elastic modulus that was close to the point of stabilization, and shape recovery could be induced, however the rubber elasticity modulus was quite low and the shape recovery speed was slow (Figure 12). For TPI:85-S:0.5, TPI:100-S:0.5 and TPI:100-S:0.75, since the elastic modulus at 37 °C was markedly decreasing and repeated crystalline melting and recrystallization was occurring (Figure 11AB), shape recovery was presumed not to be induced.

Another important theme in this study was to investigate the sealing capability of the trial material. In this study, two sealing ability tests were performed. The first used glass tubing instead of a natural root canal to allow direct observation of the behavior of the test specimen and changes in dye penetration. The internal diameter of the larger section of glass tubing was 5.5 mm, the diameter of the original test specimen was 6.0 mm (0.5 mm larger than the tube), and it was deformed to

4.6 mm (0.9 mm smaller, allowing easy insertion into the glass tube) (Figure 3A,B). Additionally, the internal diameter of the smaller section of the glass tubing was 4.3 mm, and the transition zone between these internal diameters stopped further penetration of the deformed test specimen, even if the specimen was compressed using an indenter (Figure 3A,B). In addition, natural root canals often do not have a regular tubular shape, and irregular shapes such as flattened root canals are frequently observed. Therefore, the sealing ability test was also performed using a flattened glass tube. Specimen TPI:100-S:1.25 containing the highest concentration of cross-linking agent showed the highest recovery stress (Figure 10B) and highest recovery speed (Figure 12) among all specimens showing close sealing. In addition, this test specimen could fit both the non-deformed glass tube and the flattened deformed glass tube and sealed the inner space tightly. Thus, TPI with a high cross-linking density may be suitable as a root canal filling material. Another sealing ability test using a bovine incisor was also performed, because the shape and surface properties of the bovine root canal are similar to those found in a human incisor, and bovine incisors are easy to obtain. The results of the sealing ability test using the bovine incisor indicated that, for the lateral condensation method, the apical foramen could not be sealed tightly using tug-back confirmation. For the warmed gutta-percha method, the gutta-percha fitted the root canal better than in the lateral condensation method, but leakage of dye was observed as a result of shrinkage of melted gutta-percha and extrusion of gutta-percha. The difference in dye penetration length was presumed to be mainly due to differences in the crystallization temperature and crystallization rate of the TPI [20]. For the trial point, the shape-memory effect successfully sealed the prepared root canal of the bovine incisor without use of a sealer. Additionally, as shown in Figure 15, this trial point adapted to various tapered root canal shapes without extrusion. These results suggest the applicability of the TPI based shape-memory polymer as a root canal filling material. In future studies, a trial point that can be applied to the root canal of the human tooth will be developed, it is also necessary to investigate the root canal sealer suitable for this trial point, and in addition, analysis of the stress on the tooth and the periodontal tissue by the shape-memory is also necessary for the prevention of the root fracture.

## 5. Conclusions

With the TPI-based shape-memory polymer, it was possible to recover the deformed shape under the thermal stimulus of 37 °C by the approach of increasing the proportion of CPI or cross-linking agent. However, as the proportion of CPI increased, recovery stress decreased. In contrast, as the proportion of cross-linking agent increased, recovery stress increased. The material containing the highest concentration of cross-linking agent showed superior sealing ability under a thermal stimulus of 37 °C in sealing ability tests, and it appears to be promising for application as a root canal filling material with excellent operability and sealing ability.

**Supplementary Materials:** The Supplementary Materials can be found at [www.mdpi.com/2073-4360/7/11/1512/s1](http://www.mdpi.com/2073-4360/7/11/1512/s1).

**Acknowledgments:** The authors thank Kuraray Corp. for providing TP-301. This research was supported by Grants-in-Aid for Scientific Research #14571818.

**Author Contributions:** Gakuji Tsukada and Ryuzo Kato conceived and designed the experiments; Gakuji Tsukada performed the experiments; Ryuzo Kato analyzed the data; Masayuki Tokuda and Yoshihiro Nishitani contributed reagents/materials/analysis tools; Gakuji Tsukada wrote the manuscript. All authors revised the manuscript and approved the final version.

**Conflicts of Interest:** The authors declare no conflict of interest.

## References

1. Timpawat, S.; Amornchat, C.; Trisuwan, W.R. Bacterial coronal leakage after obturation with three root canal sealers. *J. Endod.* **2001**, *27*, 36–39. [[CrossRef](#)] [[PubMed](#)]

2. Kaya, B.U.; Kececi, A.D.; Berri, S. Evaluation of the sealing ability of gutta-percha and thermoplastic synthetic polymer-based systems along the root canals through the glucose penetration model. *Oral Surg. Oral Med. Oral Pathol. Oral Radiol. Endod.* **2007**, *104*, e66–e73. [[CrossRef](#)] [[PubMed](#)]
3. Brothman, P. A comparative study of the vertical and lateral condensation of gutta-percha. *J. Endod.* **1981**, *7*, 27–30. [[CrossRef](#)]
4. Mann, S.R.; McWalter, G.M. Evaluation of apical seal and placement control in straight and curved canals obturated by laterally condensed and thermoplasticized gutta-percha. *J. Endod.* **1987**, *13*, 10–17. [[CrossRef](#)]
5. Canalda-Sahli, C.; Berástegui-Jimeno, E.; Brau-Aguadé, E. Apical sealing using two thermoplasticized gutta-percha techniques compared with lateral condensation. *J. Endod.* **1997**, *23*, 636–638. [[CrossRef](#)]
6. Sobhnamayan, F.; Sahebi, S.; Moazami, F.; Borhanhaghighi, M. Comparison of apical sealing ability of lateral condensation technique in room temperature and body-stimulated temperature (An *in vitro* study). *J. Dent. Shiraz Univ. Med. Scien.* **2013**, *14*, 25–30.
7. Allison, D.A.; Michelich, R.J.; Walton, R.E. The influence of master cone adaptation on the quality of the apical seal. *J. Endod.* **1981**, *7*, 61–65. [[CrossRef](#)]
8. Johnson, W.B.; Okla, T. A new gutta-percha technique. *J. Endod.* **1978**, *4*, 184–188. [[CrossRef](#)]
9. Moreno, A.; Mexico, M. Thermomechanically softened gutta-percha root canal filling. *J. Endod.* **1977**, *3*, 186–188. [[CrossRef](#)]
10. Schilder, H. Filling root canals in three dimensions. *Dent. Clin. North Am.* **1967**, *11*, 723–744. [[CrossRef](#)] [[PubMed](#)]
11. Yee, F.S.; Marlin, J.; Kradow, A.A.; Gron, P. Three-dimensional obturation of the root canal using injection-molded, thermoplasticized dental gutta-percha. *J. Endod.* **1977**, *3*, 168–174. [[CrossRef](#)]
12. Clinton, K.; Himel, V.T. Comparison of a warm gutta-percha obturation technique and lateral condensation. *J. Endod.* **2001**, *27*, 692–695. [[CrossRef](#)] [[PubMed](#)]
13. Weller, R.N.; Kimbrough, W.F.; Anderson, R.W. A comparison of thermoplastic obturation techniques: Adaptation to the canal walls. *J. Endod.* **1997**, *23*, 703–706. [[CrossRef](#)]
14. Lacombe, J.S.; Campbell, A.D.; Hicks, M.L.; Pelleu, G.B. A comparison of the apical seal produced by two thermoplasticized injectable gutta-percha techniques. *J. Endod.* **1988**, *14*, 445–450. [[CrossRef](#)]
15. Hata, G.-I.; Kawazoe, S.; Toda, T.; Weine, F.S. Sealing ability of thermal with and without sealer. *J. Endod.* **1992**, *18*, 322–326. [[CrossRef](#)]
16. Skinner, R.L.; Himel, V.T. The sealing ability of injection-molded thermoplasticized gutta-percha with and without the use of sealers. *J. Endod.* **1987**, *13*, 315–317. [[CrossRef](#)]
17. Evans, J.T.; Simon, J.H.S. Evaluation of the apical seal produced by injected thermoplasticized gutta-percha in the absence of smear layer and root canal sealer. *J. Endod.* **1986**, *12*, 101–107. [[CrossRef](#)]
18. Schilder, H.; Goodman, A.; Aldrich, W. The thermomechanical properties of gutta-percha: Part V. Volume changes in bulk gutta-percha as a function of temperature and its relationship to molecular phase transformation. *Oral Surg. Oral Med. Oral Pathol.* **1985**, *59*, 285–296. [[CrossRef](#)]
19. Lee, C.Q.; Chang, Y.; Cobb, C.M.; Robinson, S.; Hellmuth, E.M. Dimensional stability of thermosensitive gutta-percha. *J. Endod.* **1997**, *23*, 579–582. [[CrossRef](#)]
20. Tsukada, G.; Tanaka, T.; Torii, M.; Inoue, K. Shear modulus and thermal properties of gutta percha for root canal filling. *J. Oral. Rehabil.* **2004**, *31*, 1139–1144. [[CrossRef](#)] [[PubMed](#)]
21. Peng, L.; Ye, L.; Tan, H.; Zbou, X. Outcome of root canal obturation by warm gutta-percha *versus* cold lateral condensation: A meta-analysis. *J. Endod.* **2007**, *33*, 106–109. [[CrossRef](#)] [[PubMed](#)]
22. Al-Dewani, N.; Hayes, S.J.; Dummer, P.M.H. Comparison of laterally condensed and low-temperature thermoplasticized gutta-percha root fillings. *J. Endod.* **2000**, *26*, 733–738. [[CrossRef](#)] [[PubMed](#)]
23. Friedman, C.M.; Sandrik, J.L.; Heuer, M.A.; Rapp, G.W. Composition and mechanical properties of gutta-percha endodontic points. *J. Dent. Res.* **1975**, *54*, 921–925. [[CrossRef](#)] [[PubMed](#)]
24. Marciano, J.; Michailesco, P.M. Dental Gutta-percha: Chemical composition, X-ray identification, enthalpic studies, and clinical implication. *J. Endod.* **1989**, *15*, 149–153. [[CrossRef](#)]
25. Gurgel-Filho, E.D.; Feitosa, J.P.A.; Teixeira, F.B.; de Paula, R.C.M.; Silva, J.B.A.; Souza-Filho, F.J. Chemical and X-ray analyses of five brands of dental gutta-percha cone. *Int. Endod. J.* **2003**, *36*, 302–307. [[CrossRef](#)] [[PubMed](#)]
26. Spangberg, L.; Langeland, K.; Conn, F. Biologic effects of dental materials: 1. Toxicity of root canal filling materials on HeLa cells *in vitro*. *Oral Surg.* **1973**, *35*, 402–414. [[CrossRef](#)]

27. Pascon, E.A.; Spångberg, L.S.W. *In vitro* cytotoxicity of root canal filling materials: 1. Gutta-percha. *J. Endod.* **1990**, *16*, 429–433. [[CrossRef](#)]
28. Goodman, A.; Schilder, H.; Aldrich, W. The thermomechanical properties of gutta-percha: 2. The history and molecular chemistry of gutta-percha. *Oral Surg.* **1974**, *37*, 954–961. [[CrossRef](#)]
29. Davies, C.K.L.; Long, O.E. Morphology of *trans*-1, 4-polyisoprene crystallized in thin films. *J. Mater. Sci.* **1977**, *12*, 2165–2183. [[CrossRef](#)]
30. Yoshikawa, R. Transpolyisoprene. *J. Soc. Rubber Ind.* **1984**, *57*, 723–727. [[CrossRef](#)]
31. Ishii, M. Shape memory plastics: Polyisoprene based plastics. *Plastic Age* **1989**, *35*, 158–164.
32. Tsukada, G.; Tokuda, M.; Torii, M. Temperature triggered shape memory effect of transpolyisoprene-based polymer. *J. Endod.* **2014**, *40*, 1658–1662. [[CrossRef](#)] [[PubMed](#)]
33. Liu, C.; Qin, H.; Mather, P.T. Review of progress in shape-memory polymers. *J. Mater. Chem.* **2007**, *17*, 1543–1558. [[CrossRef](#)]
34. Small, W.; Singhal, P.; Wilson, T.S.; Maitland, D.J. Biomedical applications of thermally activated shape memory polymers. *J. Mater. Chem.* **2010**, *20*, 3356–3366. [[CrossRef](#)] [[PubMed](#)]
35. Hu, J.L.; Zhu, Y.; Huang, H.; Lu, J. Recent advances in shape-memory polymers: Structure, mechanism, functionality, modeling and applications. *Prog. Polym. Sci.* **2012**, *37*, 1720–1763. [[CrossRef](#)]
36. Guo, J.; Wang, Z.; Tong, L.; Lv, H.; Liang, W. Shape memory and thermo-mechanical properties of shape memory polymer/carbon fiber composites. *Compos. Part A* **2015**, *76*, 162–171. [[CrossRef](#)]
37. Ebara, M. Shape-memory surfaces for cell mechanobiology. *Sci. Technol. Adv. Mater.* **2015**, *16*, 1–13. [[CrossRef](#)]
38. Dow, P.R.; Ingle, J.I. Isotope determination of root canal failure. *Oral Surg. Oral Med. Oral Pathol.* **1955**, *8*, 1100–1104. [[CrossRef](#)]
39. Kersten, H.W.; Moorer, W.R. Particles and molecules in endodontic leakage. *Int. Endod. J.* **1989**, *22*, 118–124. [[CrossRef](#)] [[PubMed](#)]



© 2015 by the authors; licensee MDPI, Basel, Switzerland. This article is an open access article distributed under the terms and conditions of the Creative Commons by Attribution (CC-BY) license (<http://creativecommons.org/licenses/by/4.0/>).